

Experimental and theoretical insights of functionalized hexavanadates on Na+/K+-ATPase activity; molecular interaction field, ab initio calculations and in vitro assays

Nada B Bošnjaković-Pavlović, Xiao Xu, Danijela Krstić, Jean-Michel Gillet, Yongge B Wei, Pingfan M Wu, Mirjana M Čolović, Anne M Spasojević-de Biré

▶ **To cite this version:**

Nada B Bošnjaković-Pavlović, Xiao Xu, Danijela Krstić, Jean-Michel Gillet, Yongge B Wei, et al.. Experimental and theoretical insights of functionalized hexavanadates on Na+/K+-ATPase activity; molecular interaction field, ab initio calculations and in vitro assays. Journal of Inorganic Biochemistry, 2019, 198, pp.110720. 10.1016/j.jinorgbio.2019.110720 . hal-02163805

HAL Id: hal-02163805

https://centralesupelec.hal.science/hal-02163805

Submitted on 24 Sep 2020

HAL is a multi-disciplinary open access archive for the deposit and dissemination of scientific research documents, whether they are published or not. The documents may come from teaching and research institutions in France or abroad, or from public or private research centers.

L'archive ouverte pluridisciplinaire **HAL**, est destinée au dépôt et à la diffusion de documents scientifiques de niveau recherche, publiés ou non, émanant des établissements d'enseignement et de recherche français ou étrangers, des laboratoires publics ou privés.

Experimental and theoretical insights of functionalized hexavanadates on Na^+/K^+-ATPase activity; molecular interaction field, *ab initio* calculations and *in vitro* assays

Nada Bošnjaković-Pavlović[1,2§], Xiao Xu[1,2§], Danijela Krstić[3], Jean-Michel Gillet[1,2], Yongge Wei[4], Pingfan Wu[5], Mirjana Čolović[6], Anne Spasojević-de Biré[1,2*]

[1] Université Paris-Saclay, CentraleSupélec, Campus de Paris-Saclay, 8-10 rue Joliot-Curie, 91190 Gif-sur-Yvette, France

[2] CNRS, UMR 8580, Laboratory "Structures Propriétés et Modélisation des Solides" (SPMS), Campus de Gif, 8-10 rue Joliot-Curie,91190 Gif-sur-Yvette, France

[3]Institute of Medical Chemistry, Faculty of Medicine, University of Belgrade, Serbia

[4] Department of Chemistry, Tsinghua University, 100084 Beijing, P. R. China

[5] Institute of POM-based Materials, The Synergistic Innovation Center of Catalysis Materials of Hubei Province, Hubei University of Technology, 430086 Wuhan, Hubei Province, P. R. China

[6] Department of Physical Chemistry, Vinča Institute of Nuclear Sciences, University of Belgrade, Serbia

e-mail: anne.spasojevic@centralesupelec.fr

* author to whom correspondence should be addressed

§ authors contribute equally

Abstract

The influence of three functionalized hexavanadates (V_6): Na_2 $[V_6O_{13}\{(OCH_2)_3CCH_3\}_2]$, $[H_2]_2$ $[V_6O_{13}\{(OCH_2)_3CCH_2OCOCH_2CH_3\}_2]$ and $[(C_4H_9)_4N]_2$ $[V_6O_{13}\{(OCH_2)_3CCH_2OOC(CH_3)_2\text{-}COOH\}_2$ on Na^+/K^+-ATPase activity, was investigated *in vitro*. Including compounds already tested by Xu *et al.* (Journal of Inorganic Biochemistry 161 (2016) 27–36), all functionalized hexavanadates inhibit the activity of Na^+/K^+-ATPase in a dose-dependent manner but with different inhibitory potencies. Na_2 $[V_6O_{13}\{(OCH_2)_3CCH_3\}_2]$ was found to have the best inhibition properties - showing 50 % inhibition $IC_{50} = 5.50 \times 10^{-5}$ M, while $[(C_4H_9)_4N]_2$ $[V_6O_{13}\{(OCH_2)_3CCH_2OOC(CH_3)_2\text{-}COOH\}_2]$ showed the lowest inhibitory power, $IC_{50} = 1.31 \times 10^{-4}$ M. In order to understand the bioactivity of functionalized hexavanadates serie, we have also used a combined theoretical approach: determination of electrostatic potential from *ab initio* theoretical calculations and computation of the molecular interaction field (MIF) surface.

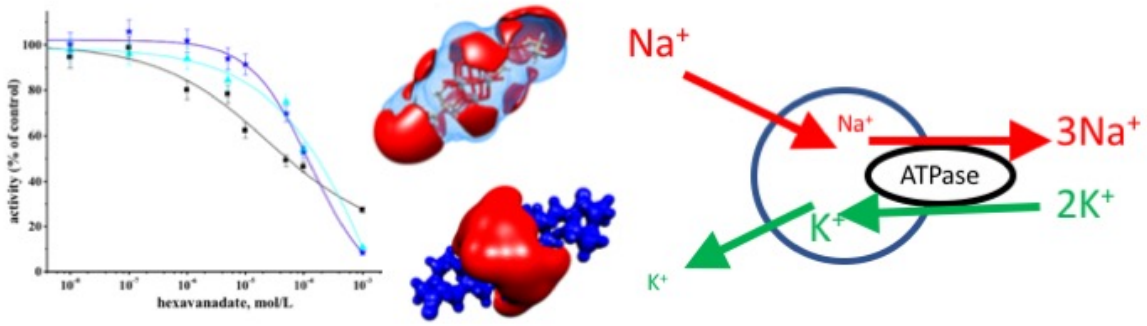
Highlights

- Functionalized hexavanadates inhibit Na^+/K^+-ATPase in a concentration-dependent manner.
- Na_2 $[V_6O_{13}\{(OCH_2)_3CCH_3\}_2]$ is the strongest investigated hexavanadates inhibitor.
- Negative electrostatic potential is an indicator of inhibition character.
- Molecular interaction field surface allows predictions of inhibition character.
- The largest negative molecular interaction field concerns the nitro- hexavanadate.

Key-words

Functionalized hexavanadate, Na^+/K^+-ATPase, Inhibition, Electrostatic potential, Molecular Interaction Field

Graphical abstract



The inhibition character on Na^+/K^+-ATPase of three functionalized hexavanadates have been determined. Using *ab-initio* calculations and molecular interaction field five criteria have been established to understand the inhibition potentiality of nine functionalized hexavanadates. The best criterion is the ratio of negative area of molecular interaction field over its molecular surface.

1. Introduction

Polyoxovanadates (POVs) is a rapidly growing family of vanadium oxide molecular anions, as attested by the occurrence progression in Web of Knowledge© (Figure S1). They exhibit interesting structures and offer extensive potential applications in material science and medicinal chemistry [1-11]. Polyoxometallates (POMs) possess important biological and pharmacological attributes such as antiviral, antibacterial and anticancer properties which are most probably based on their interactions with diverse biomacromolecules [12-17]. The Lindquist type alcohol hexavanadates (that we should refer to as V_6) are the largest subclass of the POV derivatives, in which the hexavanadate core $\{V_6O_{19}\}$ is stabilized by tridentate ligands $(OCH_2)_3R$ (R = $-CCCH_3$, $-CNO_2$, $-CCH_2OH$, ...). The pioneer investigations of these derivatives were mainly conducted by Zubieta [18-20] and Müller [21]. In recent years, some functionalized V_6 have been synthesized [22-25].

The biological activity of decavanadate (V_{10}) had been extensively reviewed [6-7, 10-11, 26] with potential use in anticancer [27-28] anti-diabetic therapies [29-30] and antibacterial activity [31]. V_{10} is known to modulate the activity of many proteins such as phosphatases [32], myosin [33-34] and calcium pump ATPase [35-36] and to interact with proteins such as actin [26, 37, 38]. New POVs have antifungal activities against Candida species [39-40].

The most frequent interactions between POMs and biomacromolecules are electrostatic interactions and hydrogen bonds. Apart from the interactions between POMs and proteins, size and shape of the POM in some cases play a tremendous role [8, 41]. A key to success and further progress in this field is a detailed understanding of the protein-ligand interactions. The description of a molecule and its influence on the surroundings is useful information to explain and understand chemical reactions and bio-chemical interactions. Depending on the different fields, there are several ways to define the interaction force of a molecule with a protein or a receptor, such as lipophilicity, polarizability, electronic properties and steric interactions. An

efficient and elegant method for predicting ligand binding sites would involve the use of a molecular docking software such as GRID [42] designed by Molecular Discovery©. GRID is used to study the energetically favorable binding sites of molecules of known structures. A binding surface on a protein is understood through the definition of an interaction energy for a probe group or compound. It then allows that probe to sample all possible sites on the surface of the protein until a set of potential energy minima is found. As a consequence, these minima represent sites at which the probe could react favorably with the protein under study [43].

Recently, we have found that POVs exhibit inhibitory influence on Na^+/K^+-ATPase activity [44-45] which is a cell membrane located enzyme. Such enzyme establishes and maintains the high internal K^+ and low internal Na^+ concentrations, characteristic and essential for normal cellular activities of most animal cells [46-47]. The activity of this enzyme is very sensitive to the presence of some metal ions and organic compounds of various structures, especially some drugs and pesticides [48-51]. Inhibitions of several ATPases such as P-type ATPases, ABC-ATPases and ribonucleases by decavanadate suggest that V_{10} interactions with these proteins are probably favored by the existence of an ATP binding site [52-54]. Considering the key role of Na^+/K^+- ATPase in normal functioning of most animal cells, as well as its pivotal role in cancer cell migration, the aim of this work is to examine the influence of three hexavanadates (namely: Na_2 $[V_6O_{13}\{(OCH_2)_3CCH_3\}_2]$ as referred to compound (**1-Na**) [20], $[H_2]_2$ $[V_6O_{13}\{(OCH_2)_3CCH_2OCOCH_2CH_3\}_2]$ (**2-H**) [55] and $[(C_4H_9)_4N]_2$ $[V_6O_{13}\{(OCH_2)_3CCH2OOC(CH_2)_2\text{-}COOH\}_2]$ (**3-TBA**) [56] where TBA $[(C_4H_9)_4N]$ is the counter cation) on Na^+/K^+- ATPase activity, using commercially available Na^+/K^+- ATPase from porcine cerebral cortex as a model system. Numbering of the compounds indicates the different functionalization (different anions), while the counterions are indicated when necessary (see abbreviation section).

In this paper, we suggest a combined approach to investigate the reactivity and to understand the bioactivity of functionalized V_6 serie involving the theoretical electrostatic potential (EP) from *ab initio* theoretical calculation, and molecular interaction field (MIF) determination. In a previous paper [45], we have studied the reactivity of four V_6 anions (**2**, **3**, **8**, **9**) using the electrostatic potential values at the molecular surface. In the present work, we have determined EP values at the molecular surface of the other functionalized V_6 serie (**5**, **6**, **7**). For all V_6 anions (**1** to **9**) and V_{10} anion (**10**) (see table S1 in supporting information) we have calculated the stabilization energy from *ab initio* calculation and determined the MIF. Understanding protein-ligand interactions is essential in drug design. Therefore, experimental results will be compared with theoretical ones generated from the molecular docking software GRID in order to determine if our methods suggest similar binding ways *i.e.* position and orientation of the ligand.

2. Materials and methods

2.1. Preparation of V_6 solutions

Synthesis of **1-Na** has been published by Chen *et al.* [20], **2-H** by Wu *et al.* [55] and **3-TBA** by Xiao *et al.* [56]. Stock solution (0.1M) of **3-TBA** was prepared by dissolving the solid compound in DMSO, while **1-Na** and **2-H** stock solutions were prepared in water. Working solutions were prepared daily by diluting the stock solutions with water to the desired concentrations, shortly before use.

2.2. Na^+/K^+-ATPase assay

Na^+/K^+-ATPase from porcine cerebral cortex was purchased from Sigma Chemicals Co.® (Germany). Final DMSO volume fraction in the incubation medium did not exceed 1%. The activity of Na^+/K^+- ATPase was followed in the absence (control) and presence (during 20 min)

of increasing V_6 concentrations by monitoring spectrophotometrically (Perkin Elmer® Lambda 35 UV-VIS spectrophotometer) the released P_i liberated from the enzymatic hydrolysis of ATP [57].

2.3. Computational details: Ab initio calculations

Density functional theory (DFT) calculations were performed with Gaussian 09 (EM64L-G09RevC.01) [58]. Different functionals and basis sets have been employed (Table S2) depending on the calculation (EP or charges). All belong to the hybrid functionals family, and therefore include a mixture of Hartree-Fock exchange with DFT exchange-correlation (B3LYP [59], M06/M06-2X [60], B3PW91 [61]). The basis sets take into account polarization and diffuse functions (6-31+G(d, p) [62], 6-311+G(d, p) / 6-311++G(d, p) [63], cc-pVTZ [64]). The atomic coordinates of **10** [65], **9** [66], and **3**[67] anions are obtained from the corresponding high resolution X-ray diffraction nuclei positions, without geometrical optimization. Atomic coordinates of other V_6 serie are obtained from Cambridge Structure Database (CSD). Refcodes and references are given in Table S1. The geometry has been optimized within the M06/6-31+G(d, p) quantum chemical model. The computed densities have converged at cc-pVTZ level, except for **5**, which has converged at 6-311+G(d, p) level because of computation time constraints. Due to disorder on one organic chain, no EP has been determined for **3**. Only a density has been computed in order to estimate the volume and the area at the molecular surface. All figures have been obtained using Molekel [68].

Converged *ab-initio* results are then used to compute topological properties and indicators in in the framework of Bader's Quantum Theory of Atoms in Molecules theory using a dedicated computer code AIMALL (Version 14.11.23) [69].

2.4. Computational details: molecular interaction field

The interaction of the probe group (H_2O, OH, NH, CH_3, metal,...) with the target (the drug or the inhibitor) is computed at sample positions (the grid points) distributed throughout and around the molecule [42]. With the probe at each GRID [70] point in turn, the total interaction energy is calculated from:

$$\sum E = E_{LJ} + E_Q + E_{HB} + E_S$$

Eq. (1)

In this formula:

- $\sum E$ indicates pairwise energy summation between the probe at its grid points and every appropriate atom of the target (including predicted water molecules);

- E_S is the appropriate entropic term at the grid points introduced by the authors [71] to take into account when parts of the target are treated as flexible or when the probe interactions are compared to that of water, and for the hydrophobic probe;

- The E_{LJ} term is the well-known "Lennard-Jones energy", and is computed as the sum of two terms:

$$E_{LJ} = \frac{A}{d^{12}} - \frac{B}{d^6}$$

Eq. (2)

d is the inter-atomic distance, and the energy variables A and B are calculated from the Van der Waals radius, polarizability and effective number of electrons of the atoms ($E_{LJ} = E_{VDWR}$);

- E_Q is the electrostatic term and E_{HB} is the standard hydrogen bond interaction.

We used an unstable development release of GRID software [70] to parametrize V^{2+} in the target, due to the fact that the commercial version is only configured for vanadium as a probe. The impossibility to constrain the total charge on the molecules implies that the results mapped on the molecular surface (as determined from *ab initio* calculations) are presented in arbitrary unit (a.u.) which should be $kcal.mol^{-1}$. The figures presented in this paper have been done using Chimera [UCSF Chimera, version 1.13.1].

3. Results and discussions

3.1. In vitro influence of V_6 compounds on Na^+/K^+- ATPase activity

In a previous paper [45], we have studied *in vitro* influence of five functionalized V_6 (**1-TBA, 2-TBA, 7-TBA, 8-TBA** and **8-Na**) on the commercial porcine cerebral cortex Na^+/K^+- ATPase activity. In this study, the influence of three other functionalized V_6 compounds (**1-Na, 2-H**, **3-TBA**) on Na^+/K^+- ATPase activity was investigated in the concentration range 1×10^{-8} - 1×10^{-3} M. The enzyme activity, expressed as a percentage of the control value (obtained without inhibitor), decreases in the presence of increasing V_6 concentrations, showing a monophasic sigmoidal curve for all cases (Figure 1a).

The inhibition parameters, the concentration of the investigated compounds with capability to inhibit 50 % of the enzyme activity after given exposure time (IC_{50}) and Hill's coefficient (n_H), were determined using the Hill's analysis (Figure 1b) and are summarized in Table 1. Our results indicate that all investigated compounds inhibit the Na^+/K^+ ATPase activity in a dose-dependent manner, but with different inhibiting potencies. **1-Na** (IC_{50} = 5.50 × 10^{-5} M) was found to be the best inhibitor of Na^+/K^+ ATPase activity, while **3-TBA** showed the lowest inhibitory potency (IC_{50} = 1.31 × 10^{-4} M) (Table1). The calculated n_H values ($n_H < 1$) suggest that there is no positive cooperativity inV_6 binding relative to the enzyme (see Table 1).

Those results are in agreement with the concentration-dependent inhibitory effect of POVs on synaptic plasma membrane and commercially available porcine cerebral cortex Na^+/K^+ ATPase already reported [44-45]. Table 2 contains the inhibition results for eight investigated V_6 (three compounds in this work and five ones previously reported); the counterion is indicated. Our results demonstrate that the inhibitory effect on Na^+/K^+-ATPase activity leads to the following ranking: **7-TBA** > **8-TBA** > **1-TBA** > **2-TBA** > **1-Na** ~ **2-H** > **3-TBA** > **8-Na**. As a matter of fact, the most potent inhibitor is compound **7-TBA** (IC_{50} = (1.8 ± 0.5) × 10^{-5} M), while the

compounds **8-TBA**, **1-Na**, **2-TBA** and **1-TBA** are significantly weaker inhibitors of Na^+/K^+-ATPase. Three anions have been tested with different counter cations: **1-TBA**, **2-TBA** and **8-TBA** with TBA, while **1-Na** and **8-Na** where prepared with $[Na]^+$; and **2-H** with $[H]^+$. It is interesting to observe that both compounds **8-TBA** and **2-TBA**, synthesized with TBA as a counter cation, have lower IC_{50}. The last compound **1-Na** is in the interval errors. This would suggest that small cations such as sodium or proton could interact with Na^+/K^+- ATPase and prevent the inhibition action of V_6. Therefore, taking into account the inhibition parameter with the same counter cation (TBA), we observe the following ranking: **7-TBA** > **8-TBA** > **1-TBA** > **2-TBA** > **3-TBA**. From simple chemical eyes, it seems that an additional negative charge on nitro- **7-TBA** or alcoholic groups **8-TBA** results in stronger enzyme inhibition. **10-NH_4** is up to approximately two hundred times more potent inhibitor of the purified enzyme (IC_{50} = 1.71 × 10^{-6} M) [44] than the investigated V_6 compounds. This is in agreement with the fact that all the functionalized V_6 anions bear a formal charge of -2, while V_{10} is described with a formal charge of -6. The experimental electron density determination on **2-TBA** in solid state, and its interpretation *via* integrated source function, give only 5.5 % of charge transfer from cation to anion [67]. In solution state, the functionalized V_6 and V_{10} anions are stable [72].

Although a few different isoforms of brain Na^+/K^+-ATPase have been known [44], the obtained monophasic inhibition curves do not suggest the heterogeneity of the V_6 binding sites. This is in agreement with previously published findings related to POM-induced inhibition of different types of ATPases [44-45, 51].

Hexavanadate $V^{(V)}$ derivatives are susceptible to hydrolysis and not stable in water [73]. When the valence state involves (V^{4+}) species, it comes to be stable against hydrolysis. It should be no problem because the activity is far below the decavanadates and this decomposition should be minor.

3.2. Ab initio calculations

In order to interpret the differences we have observed in inhibition activities of POVs and so as to complete our investigation, *ab initio* calculations (the energy of stabilization and theoretical EP) were carried out for different V_6 anions (Table S2).

Reactivities of four V_6 anions (**1**, **2**, **7** and **8**) using EP values at the molecular surface have already been investigated in a previous work [45]. We have now determined EP values at the molecular surface of the other functionalized V_6 anions (**4**, **5**, **6** and **9**) and for the V_{10} anion (**10**). The quality of these *ab initio* calculations is established through the comparison of the experimental EP mapped on the molecular surface of **10** determined previously [65] with the theoretical one (Figure 2, first line). The excellent agreement brings legitimacy to a precise interpretation of *ab initio* results on the V_6 serie.

In order to graphically exhibit the intermolecular charge transfer, between V_6 core and the organic ligand, iso-surfaces of EP are mapped (iso-value surface at ± 0.40 $eÅ^{-1}$) for anions **1** (Figure 3), **7** (Figure 4), **2** (Figure 5), **9** (Figure 6), **6** (Figure S3), **4** (Figure S4), **5** (Figure S5), **8** (Figure S6). The qualitative observation of the EP indicates that V_6 have two hydrophobic heads and an hydrophilic hexavanadate core. The red part (negative) is localized around the V6 core, which corresponds to the most nucleophilic regions, while the blue part (positive) is concentrated over the organic ligand and represents the most electrophilic regions. The EP values are the most negative in the vicinity of the three oxygen atoms. It provides a predictable pattern for noncovalent interactions and figures out the probable chemical reaction sites. In this type of functionalized V_6 compounds, O1x (bonded to only one tungsten atom) and O2x (shared between two tungsten atoms) are potential reaction sites [21, 74, 75]. Moreover, three anions **6**, **7** and **8** present an extension of the nucleophilic region on the organic chain. These negative regions are in the vicinity of heteroatoms (oxygen or carbon). A selection of quantitative parameters is reported in Table 2. This extension is not directly connected to the number of

heteroatoms on the organic chain, but it is the signature of amino-, nitro-, hydroxy, pyridyl-chemical groups. Compounds which present an ester group do not exhibit negative EP in the vicinity of their oxygen atoms. In order to explain the differences in term of inhibition for the compounds studied in this paper, we make the hypothesis that a negative contribution will favorize inhibition. Therefore, in the following discussion we will examine some criteria which could have an impact on their inhibition potencies. According to the criterion, "a negative EP extension surface on the organic chain" that we will refer to as criterion I, anions **6**, **7** and **8** would be better inhibitors than the others (no results on **5**).

Atomic net charges are obtained for short and long functionalized V_6 serie by integration on atomic basins following the method of QTAIM (Table S3). Charges of V atoms are in a narrow range, from +2.333 e to +2.483 e. Summations of AIM charges for V_6 core are maintained around -5.2 e although the organic ligands are chemically different. Therefore, the criterion "theoretical atomic net charges values" that we will refer to as criterion II, would not be a pertinent criterion for explaining the different inhibition values for the V_6 serie.

3.3. Molecular interactions field calculation

MIF surfaces for seven V_6 and for V_{10} indicating the place of preferential interactions between vanadate and water have been determined. MIF values are presented as positive and negative iso-surfaces (second line, left of the figure) and are also plotted on the molecular surface (second line, right of the figure) for the following anions: **1** (Figure 3), **7** (Figure 4), **2** (Figure 5), **9** (Figure 6), **6** (Figure S3), **4** (Figure S4), **5** (Figure S5) and **10** (Figure 2). Iso-surface positive MIF (in red on the figures) mimic the possible interaction localization between protons of the active site of the Na^+/K^+-ATPase and functionalized V_6. According to the criterion, "a negative MIF extension on the organic chain", that we will refer to as III, anions **6**, **7**, **2**, **9** and **4** would be better inhibitors than the others.

In order to quantify the extension of these surfaces, volumes and areas (at the values indicated in the Figures) are reported in Table 2. A larger surface would be favorable to interactions. According to the criterion, "a MIF surface area value" that we will refer to as IV, V_6 serie could be ranked as follows: **9** >> **10** >> **4** > **5** ~ **6** ~ **2** >> **1**. It leads to the prediction that **9** would be the best inhibitor (no results on **8** and **3**).

In Figure 2, the EP mapped on molecular surface of **10** gives a range of colors leading us to distinguish the different oxygen atoms and determine which oxygen atom would be preferentially involved in the interaction (in solid state as well as in solution state) [76]. In contrast to MIF mapped on the same molecular surface, differences cannot be distinguished between the oxygen atoms of V_{10}. For the V_6 compounds, the molecular surface is divided into two areas: the positive MIF (blue part) and the negative MIF (red part). There is no smooth transition between these two areas. However, as for EP, the values of MIF (Figure S3, second line left and right) at greater distance (as depicted by the iso-surface) indicates the contribution of nitrogen atom to the prediction of interaction (see for example compound **7**).

3.4. Interpretation of the inhibition results combining EP and MIF results

According to the three methods (IC_{50}, EP, MIF) used in this paper to study the potential inhibiting power of POVs on Na^+/K^+-ATPase activity, we have been able to draw some conclusions which are summarized in Table 3 and presented graphically in Figure 7. As observed previously, small counter cations could bind to the protein and therefore perturbate the influence of the organic substituent on a V_6 serie. Therefore, we have decided to retain for our conclusions only the experiments performed with TBA as a cation. Their IC_{50} values are reported in orange in Figure 7. Examination of EP have been done *via* observation of negative EP extension on organic chain. Favorable criterion I is indicated in the column with the symbol (✓), while unfavorable criterion I appears in the column with the symbol (✗). This is graphically

indicated on the right part of Figure 7 (green bars). The two first better inhibitors verify criterion I. Similarly, qualitative observation of the MIF extension in the vicinity of the organic part (criterion III) is also shown on the right part of Figure 7 (red bars). There is no correlation with the inhibition behavior of the three compounds (**7-TBA**, **2-H** and **1-Na**) for which we have IC_{50} and criterion III information. Criterion IV for the V_6 serie has been reported in Table 2 and in Figure S7 (grey bars). There is still no correlation with the inhibition values.

In order to normalize this area with respect to the size of the different anions, a ratio (negative MIF iso-surface at 2 Kcal.mol^{-1} over the molecular surface area) is calculated (Table 2). Those ratios are displayed in the center of Figure 7 (blue bars) and is refer to as criterion V. Compounds have been ranked according to this ratio (top the greatest ratio, to the smallest on the bottom). The expected correlation is now rendered for the three V_6 anions (**7**, **2** and **1**) and for **10.** Those four anions are the ones for which we have both information: the greater the ratio, the better the inhibitor. In other word, it means that smaller compounds exhibiting larger negative region for interactions are expected to be better inhibitors. The last two anions for which MIF could not be computed (for technical reasons) have been placed in Figure 7 according to their IC_{50} values.

Now, we can observe the organic radical R (left part of Figure 7) from the $[V_6O_{13}\{(OCH_2)_3R\}_2]^{2-}$ anion formula. This allows us to predict which compounds would be good inhibitors. Our recommendation would be to use an amino- group on a small organic chain such as compound **6-TBA**. Comparisons between **2-TBA**, **4-TBA** and **5-TBA** indicate that a longer chain should decrease the inhibition potential. A large compound with many heteroatoms such as **5-TBA** gives a large extension of negative MIF over the organic chain, but a smaller ratio. Therefore, it should not be a good inhibitor.

4. Conclusion

From a methodological point of view, the goal of this work was to use the MIF tool as a bridge between experimental inhibition results and sophisticated CPU time consuming *ab initio* computations. Our results have demonstrated that EP iso-surface would be good criterion to classify interactions, but it did not provide any ranking. A combination of fine quantitative analysis of MIF results and *ab initio* calculations allowed us to interpret and predict the potential inhibitor character of a V_6 series.

From a biochemical point of view, we can conclude that the tested functionalized V_6 compounds exhibit concentration-dependent inhibitory effect on Na^+/K^+-ATPase activity. The inhibitory potencies of this V6 series toward Na^+/K^+-ATPase are weaker (about two orders of magnitude) related to V_{10}. Size of **10** is smaller than the functionalized V_6, which indicates that **10** can easily access to the binding site of the receptor. The most hydrophilic EP and MIF iso-surface concerns anion **7**. This small anion has negative charge around the two heads and the higher affinity toward (positively charged) protein regions. Our results confirm that the differences in the inhibition power are due to different charges, sizes and shapes of these V_6, and more precisely to the ratio of a hydrophilic region area normalized with their molecular surface area of the whole molecule.

It is well known that a monomeric orthovanadate is bound to the catalytic site of P-type ATPases, acting as a transition-state analog of phosphate, and consequently inhibits the enzyme activity at nanomolar concentrations [77, 78]. Because the investigated polymeric vanadates exhibit weaker inhibitory potencies (at micromolar concentrations), it seems that the enzyme active site is not directly involved in the inhibition by the polymeric species. In other words, the enzyme activity is modified due to the interaction of the polymeric vanadates with binding sites different from the active one.

A better understanding of POMs – protein interaction may be useful to elucidate the biological activities of the POMs in order to make them available and safe for clinical use. This approach, which combines *ab initio* calculations, semi-empirical computations and experimental inhibition studies, contributes to finding a potential and at the same time selective and specific Na^+/K^+-ATPase inhibitor, one of the key enzymes in the functioning of a healthy cell and development of pathological conditions.

Supporting information

Table S1. Compounds cited in this work; Table S2. Computational details tested in this work; Table S3. Theoretical AIM charge*;* Figure S1. Progression of the polyoxovanadate and hexavanadate; Figure S2. Three models of V_6 DFT calculations; Figure S3. Electrostatic potential (EP) and molecular interaction field (MIF), water probe on anion **6**; Figure S4. Electrostatic potential (EP) and molecular interaction field (MIF), water probe on anion **4**; Figure S5. Electrostatic potential (EP) and molecular interaction field (MIF), water probe on anion **5**; Figure S6. Electrostatic potential (EP) of anion **8**; Figure S7. Comparison of IC_{50} values with two criteria deduced from the MIF analysis; Figure S8. Powders of the functionalized V_6 serie.

Abbreviation

Numbering of the compounds is an association of a number (the POV anions) and a group of letters (the counter cation). When a fictive anion is concerned (for EP and MIF), the corresponding number (without letters) is given in the text.

1-Na = $Na_2\,[V_6O_{13}\{(OCH_2)_3CCH_3\}_2]$

1-TBA = $[(C_4H_9)_4N]_2\ [V_6\text{-}O_{13}\{(OCH_2)_3CCH_3\}_2]$

2-H = $[H_2]_2\ [V_6O_{13}\{(OCH_2)_3CCH_2OCOCH_2CH_3\}_2]$

2-TBA = $[(C_4H_9)_4N]_2\ [V_6O_{13}\{(OCH_2)_3CCH_2OCOCH_2CH_3\}_2]$

3-TBA = $[(C_4H_9)_4N]_2\ [V_6\text{-}O_{13}\{(OCH_2)_3CCH_2OOC(CH_3)_2COOH\}_2$

4-TBA = $[(C_4H_9)_4N]_2\ [V_6O_{13}\{(OCH_2)_3CCH_2OOC(CH_2)_4CH_3\}_2]$

5-TBA = $[(C_4H_9)_4N]_2\ [V_6O_{13}\{(OCH_2)_3CCH_2OOC(CH_2)_{16}CH_3\}_2]$

6-TBA= $[(C_4H_9)_4N]_2\ [V_6O_{13}\{(OCH_2)_3CNH_2\}_2]\cdot$

7-TBA = $[(C_4H_9)_4N]_2\ [V_6O_{13}\{(OCH_2)_3CNO_2\}_2]$

7-TBA-CH_2Cl_2 = $[(C_4H_9)_4N]_2\ [V_6O_{13}\{(OCH_2)_3CNO_2\}_2]\ 0.67(CH_2Cl_2)$

8 -TBA= $[(C_4H_9)_4N]_2\ [V_6O_{13}\{(OCH_2)_3CCH_2OH\}_2]$

8-Na = $Na_2\,[V_6O_{13}\{(OCH_2)_3CCH_2OH\}_2]$

9-TBA = $[(C_4H_9)_4N]_2\ [V_6O_{13}\{(OCH_2)_3CNHCOC_{15}N_3\}_2]$

10-NH_4 = $(NH_4)_6\,[V_{10}\,O_{28}]\,.\,5H_2O$

10-Cyt = $Na_3\,[V_{10}\,O_{28}]\,(C_4N_3OH_5)_3(C_4N_3OH_6)_3$

CSD = Cambridge Structure Database

DFT = density functional theory

EP = electrostatic potential

MIF = molecular interaction field

POM = polyoxometalate

POV = polyoxovanadate

V_{10} = decavanadate

V_6 = hexavanadate

Acknowledgement

ASdB thanks Campus France for a PHC support (Pavle Savić 23643QC) co-directed with Vesna Vasić (Institut Vinča). This project has initiated the Serbian-French collaboration presented in this paper. This work was also supported by the Ministry of Education, Science and Technological Development of the Republic of Serbia (Projects No. 172023). NBP thanks Campus France for a Prestige grant. XX thanks the Chinese Science of Council for a financial support during his PhD. YW thanks the financial support of the National Natural Science Foundation of China (NSFC Nos. 21471087, 21631007 and 21225103). ASdB, NBP and XX thank Simon Cross and Loriano Storchi from Molecular Discovery for their help in using a modifying version of GRID. ASdB and NBP thank Sladjana Novaković (invited researcher at CentraleSupelec and member of the Institut Vinča, Serbia) for her kind technical help. The authors whish to thank the referees for their pertinent comments.

List of softwares

GRID

Gaussian 09

Molekel

AIMALL

Chimera

References

[1] M.T. Pope, A. Muller, Polyoxometalates: From Platonic Solids to Anti-Retroviral Activity, Kluwer, Dordrecht, 1994.

[2] C. Hill, Introduction: Polyoxometalates Multicomponent Molecular Vehicles To Probe Fundamental Issues and Practical Problems, Chem. Rev. 98, (1998), 1–390. https://doi.org/10.1021/cr960395y

[3] M. Aureliano, R.M.C. Gândara, Decavanadate effects in biological systems, J. Inorg. Biochem. 99 (2005) 979–985. https://doi.org/10.1016/j.jinorgbio.2005.02.024.

[4] M. Aureliano, Decavanadate: a journey in a search of a role, Dalton Trans**.** (2009) 9093–9100. https://doi.org/10.1039/B907581J

[5] M. Aureliano, D.C. Crans, Decavanadate $(V_{10}O_{28})^{6-}$ and oxovanadates: Oxometalates with many biological activities, J. Inorg. Biochem. 103 (2009) 536–546. https://doi.org/10.1016/j.jinorgbio.2008.11.010.

[6] M. Aureliano, A. Ohlin, Decavanadate in vitro and in vivo effects: facts and opinions, J. Inorg. Biochem. 137 (2014) 123–130. https://doi.org/10.1016/j.jinorgbio.2014.05.002.

[7] M. Aureliano, Decavanadate contribution to vanadium biochemistry: *In vitro* and *in vivo* studies, Inorg. Chim. Acta 420 (2014) 4–7. https://doi.org/10.1016/j.ica.2013.10.010.

[8] A. Bijelic, A. Rompel, The use of polyoxometalates in protein crystallography – An attempt to widen a well-known bottleneck, Coord. Chem. Rev. 299 (2015) 22–38. https://doi.org/10.1016/j.ccr.2015.03.018.

[9] K.Y. Monakhov, W. Bensch, P. Kogerler, Semimetal-functionalised polyoxovanadates, Chem. Soc. Rev., 44 (2015) 8443–8483. http://dx.doi.org/10.1039/C5CS00531K.

[10] J. C. Pessoaa, S. Etcheverry, D. Gambinoc, Vanadium compounds in medicine, Coord. Chem. Rev. 301–302 (2015) 24–48. https://doi.org/10.1016/j.ccr.2014.12.002.

[11] M. Aureliano, Decavanadate Toxicology and Pharmacological Activities: V10 or V1, Both or None? Oxidative Medicine and Cellular longevity 2016 (3):1-8. http://dx.doi.org/10.1155/2016/6103457.

[12] X. Wang, F. Li, S. Liu, M.T. Pope, New liposome-encapsulated polyoxometalates: synthesis and antitumoral activity. J. Inorg. Biochem. 99 (2005) 452–457. https://doi.org/10.1016/j.jinorgbio.2004.10.020.

[13] A. Seko, T. Yamase, K. Yamashita, Polyoxometalates as effective inhibitors for sialyl- and sulfotransferases. J Inorg Biochem 103 (2009) 1061–1066. https://doi.org/10.1016/j.jinorgbio.2009.05.002.

[14] Y. Qi, Y. Xiang, J. Wang, Y. Qi, J. Li, J, Niu J. Zhong, Inhibition of hepatitis C virus infection by polyoxometalates, Antiviral Res. 100 (2013) 392–398. https://doi.org/10.1016/j.antiviral.2013.08.025.

[15] X.G. Yang, X.D. Yang, L. Yuan, K. Wang, D.C. Crans, The Permeability and Cytotoxicity of Insulin-Mimetic Vanadium Compounds, Pharm. Res. 21 (2004) 1026–1033. https://doi.org/10.1023/B:PHAM.0000029293.89113.d5.

[16] M.S. Molinuevo, D.A. Barrio, A.M. Cortizo, S.B. Etcheverry, Antitumoral properties of two new vanadyl (IV) complexes in osteoblasts in culture: Role of apoptosis and oxidative stress, Cancer Chemother. Pharmacol. 53 (2004) 163–172. https://doi.org/10.1007/s00280-003-0708-7.

[17] R.K. Mitra, P.K. Verma, D. Wulferding, D. Menzel, T. Mitra, A.M. Todea, P. Lemmens, A. Mller, S.K. Pal, A Molecular Magnet Confined in the Nanocage of a Globular Protein, ChemPhysChem 11 (2010) 389–393. https://doi.org/10.1002/cphc.200900708.

[18] Q. Chen, J. Zubieta, Synthesis and structural characterization of a polyoxovanadate coordination complex with a hexametalate core: $[(n\text{-}C_4H_9)_4N]_2[V_6O_{13}\{O_2NC(CH_2O)_3\}_2]$, Inorg. Chem. 29 (1990) 1456-1458. https://doi.org/10.1021/ic00333a002.

[19] Q. Chen, D.P. Goshorn, C.P. Scholes, X.L. Tan, J. Zubieta, Coordination compounds of polyoxovanadates with a hexametalate core. Chemical and structural characterization of $[V^{V}_{6}O_{13}[(OCH_2)_3CR]_2]^{2-}$, $[V^{V}_{6}O_{11}(OH)_2[(OCH_2)_3CR]_2]$ $[V^{IV}_{4}V^{V}_{2}O_9(OH)_4[(OCH_2)_3CR]_2]^{2-}$, and $[V^{IV}_{6}O_7(OH)_6](OCH_2)_3CR]_2]^{2-}$, J. Am. Chem. Soc. 114 (1992) 4667–468. https://doi.org/10.1021/ja00038a033.

[20] Q. Chen, J.A. Zubieta, Structural investigations of the hexavanadium core $\{V_6O_{19}\}$ in 'oxidized', mixed valence and 'reduced' clusters of the type $[V^{V}_{6-n}V^{IV}_{n}$ $O_{13-n}(OH)_n\{(OCH_2)_3CR\}_2]^{2-}$, n=0, 3 and 6, Inorg. Chim. Acta 198–200 (1992) 95–100. https://doi.org/10.1016/S0020-1693(00)92350-8.

[21] A. Müller, J. Meyer, H. Bögge, A. Stammler, A. Botar, Cis-/Trans-Isomerie bei Bis-(trisalkoxy)-hexavanadaten: cis-$Na_2[V^{IV}_{6}O_7(OH)_6\{(OCH_2)_3CCH_2OH\}_2]$ · 8 H_2O, cis-$(CN_3H_6)_3[V^{IV}V^{V}_{5}O_{13}\{(OCH_2)_3CCH_2OH\}_2]$ · 4,5 H_2O und *trans*-$(CN_3H_6)_2[V^{V}_{6}$ $O_{13}\{(OCH_2)_3CCH_2OH\}_2]$ · H_2O, Z. Anorg Allg Chem 621 (1995) 1818–1831. https://doi.org/10.1002/zaac.19956211103.

[22] P. Yin, A. Bayaguud, P. Cheng, F. Haso, L. Hu, J. Wang, D. Vezenov, R.E. Winans, J. Hao, T. Li, Y. Wei, T. Liu, Spontaneous Stepwise Self-Assembly of a Polyoxometalate–Organic Hybrid into Catalytically Active One-Dimensional Anisotropic Structures, Chem. Eur. J. 20 (2014) 9589–9595. https://doi.org/10.1002/chem.201402974

[23] J.K. Li, C.W. Hu. Progress in Polyoxovanadate Chemistry, Chinese J Inorg Chem 31 (2015) 1705–1725. htpps://doi.org/10.11862/CJIC.2015.247

[24] A. Bayaguud, J.D. Li, S. She, Y. Wei, A simple synthetic route to polyoxovanadate-based organicinorganic hybrids using EEDQ as an ester-coupling agent, Dalton Trans. 46 (2017) 4602-4608. https://doi.org/10.1039/C7DT00274B.

[25] B. Huang, Z. Xiao, B. Wu, X. Hu, X. Hu, P. Wu, Y. Wei, Synthesis, crystal structure and spectroscopic studies of a series of hexavanadate hybrids with multiple functional groups,

Inorg. Chem. Front. 4 (2017) 165–170. http://dx.doi.org/10.1039/C6QI00302H.

[26] S. Ramos, J. J. G. Moura and M. Aureliano, Recent advances into vanadyl, vanadate and decavanadate interactions with actin, Metallomics, 4 (2012) 16–22. https://doi.org/10.1039/C1MT00124H.

[27] E. Kioseoglou, S. Petanidis, C. Gabriel, A. Salifoglou, The chemistry and biology of vanadium compounds in cancer therapeutics, Coord. Chem. Rev. 301–302 (2015) 87–105. https://doi.org/10.1016/j.ccr.2015.03.010

[28] E. Sánchez-Lara, S.Treviño, B.L Sánchez-Gaytán, E. Sánchez-Mora, M. Eugenia Castro, F.J. Meléndez-Bustamante, M.A. Méndez-Rojas, E. González-Vergara, Decavanadate Salts of Cytosine and Metformin: A Combined Experimental-Theoretical Study of Potential Metallodrugs Against Diabetes and Cancer, Front Chem 6 (2018) 402, https://doi.org/10.3389/fchem.2018.00402.

[29] S. Treviño, D. Velázquez-Vázquez, E. Sánchez-Lara, A. Diaz-Fonseca, J. Á. Flores-Hernandez, A. Pérez-Benítez, E. Brambila-Colombres, E. González-Vergara, Metforminium Decavanadate as a Potential Metallopharmaceutical Drug for the Treatment of Diabetes Mellitus, Oxid. Med. Cell. Longev. 2016 (2016) 6058705-6058419. http://dx.doi.org/10.1155/2016/6058705.

[30] C. Carpéné, S. Garcia-Vicente, M. Serrano, L. Marti, C. Belles, M. Royo, J. Galitzky, A. Zorzano, X. Testar, Insulin-mimetic compound hexaquis (benzylammonium) decavanadate is antilipolytic in human fat cells, World J. Diabetes 8 (2017) 143-153. https://doi.org/10.4239/wjd.v8.i4.143

[31] S. Toumi, N. Ratel-Ramond, S. Akrich, Decavanadate Cage-like Cluster Templated by Organic Counter Cation: Synthesis, Characterization and Its Antimicrobial Effect Against Gram Positive E. Feacium, J Clust Sci 26 (2015) 1821–1831. https://doi.org/10.1007/s10876-015-0881-y.

[32] T.L. Turner, V.H. Nguyen, C.C. McLauchlan, Z. Dymon, B.M. Dorsey, J.D. Hooker and M.A. Jones, Inhibitory effects of decavanadate on several enzymes and Leishmania tarentolae *in vitro*, J. Inorg Biochem., 108 (2012) 96–104, https://doi.org/10.1016/j.jinorgbio.2011.09.009.

[33] T. Tiago, P. Martel, C. Gutiérrez-Merino and M. Aureliano, Binding modes of decavanadate to myosin and inhibition of the actomyosin ATPase activity, Biochim. Biophys. Acta, 1771 (2007) 474–48. https://doi.org/10.1016/j.bbapap.2007.02.004.

[34] N. Steens, A.M. Ramadan, G. Absillis, T.N. Parac-Vogt, Hydrolytic cleavage of DNA-model substrates promoted by polyoxovanadates, Dalton Trans. 39 (2010) 585–592. http://dx.doi.org/10.1039/B913471A.

[35] G. Fraqueza, C. A. Ohlin, W. H. Casey and M. J. Aureliano, Sarcoplasmic reticulum calcium ATPase interactions with decaniobate, decavanadate, vanadate, tungstate and molybdate, J. Inorg. Biochem. 107 (2012) 82–89. https://doi.org/10.1016/j.jinorgbio.2011.10.010.

[36] G. Fraqueza, L. A. E. Batista de Carvalho, M. Paula, M. Marques, L. Maia, C.A. Ohlin, W.H. Casey, M. Aureliano, Decavanadate, decaniobate, tungstate and molybdate interactions with sarcoplasmic reticulum Ca^{2+}-ATPase: quercetin prevents cysteine oxidation by vanadate but does not reverse ATPase inhibition, Dalton Trans. 41 (2012) 12749–12758. https://doi.org/10.1039/C2DT31688A.

[37] S. Ramos, J. J.G. Moura, M. Aureliano, A Comparison between Vanadyl, Vanadate, and Decavanadate Effects in Actin Structure and Function: Combination of Several Spectroscopic Studies, Spectrosc-Int J, 5-6, 27 (2012), 355–359. http://dx.doi.org/10.1155/2012/532904.

[38] S. Ramos, M. Manuel, T. Tiago, R.M.C. Gândara, R.O. Duarte, J.J.G. Moura, C. Gutiérrez-Merino, M. Aurelian, Decavanadate interactions with actin: Inhibition of G-actin

polymerization and stabilization of decameric vanadate, J. Inorg. Biochem., 100 (2006) 1734–1743. https://doi.org/10.1016/j.jinorgbio.2006.06.007.

[39] S. Guo, W. Yang, M. Zhao. Wei, R. Tian, B. Zhang, Y. Qi, In Vitro Anticandidal Activity and Mechanism of a Polyoxovanadate Functionalized by Zn-Fluconazole Complexes, Molecules (5) 23 (2018) 1122–1133. https://doi.org/10.3390/molecules23051122.

[40] H. Li, H.W. Gong, Y.F. Qi, J. Li, X.F. Ji, J.H. Sun, R. Tian, H. Bao, X.F. Song, Q. Chen,G. Liu, *In vitro* and *in vivo* antifungal activities and mechanism of heteropolytungstates against Candida species. Sci Rep. 7 (2017) 16942 https://doi.org/10.1038/s41598-017-17239-8

[41] A. Bijelic, C. Molitor, S.G. Mauracher, R. Al-Oweini, U. Kortz, A. Rompel, Hen Egg-White Lysozyme Crystallisation: Protein Stacking and Structure Stability Enhanced by a Tellurium(VI)-Centred Polyoxotungstate, ChemBioChem, 16 (2015) 233–241. https://doi.org/10.1002/cbic.201402597.

[42] G. Cruciani, Molecular Interaction Fields: Applications in Drug Discovery and ADME Prediction. Wiley, 2006.

[43] A. Artese, S. Cross, G. Costa, G. Gruciani, Molecular interaction fields in drug discovery: Recent advances and future perspectives, Wiley interdisciplinary reviews: Computational Molecular Science. 3(6) (2013) 594-613. https://doi.org/10.1002/wcms.1150.

[44] D. Krstić, M. Čolović, N. Bošnjaković-Pavlović, A. Spasojević-de Biré, V. Vasić, Influence of decavanadate on rat synaptic plasma membrane ATPases activity, Gen. Physiol. Biophys. 28 (2009) 302–308. https://doi.org/10.4149/gpb_2009_03_302.

[45] X. Xu, N. Bošnjaković-Pavlović, M. Čolović, D. Krstić, V. Vasić, J.M. Gillet, P. Wu, Y. Wei, A. Spasojević-de Biré, A combined crystallographic analysis and ab initio calculations to interpret the reactivity of functionalized hexavanadates and their inhibitor

potency toward Na(+)/K(+)-ATPase, J. Inorg. Biochem. 161 (2016) 27–36. https://doi.org/10.1016/j.jinorgbio.2016.04.029.

[46] L.A. Vasilets, W. Schwarz, Structure-function relationships of cation binding in the Na^+/K^+-ATPase, Biochim. Biophys. Acta. 1154 (1993) 201–222, https://doi.org/10.1016/0304-4157(93)90012-D.

[47] G. Rodrigez de Lores Aranaiz, C. Pena, Characterization of synaptosomal membrane Na^+, K^+-ATPase inhibitors, Neurochem. Int. 27 (1995) 319–327. https://doi.org/10.1016/0197-0186(95)00013-X.

[48] J.Z. Blasiak, Cooperative Binding of the Organophosphate Paraoxon to the (Na+ + K+)-ATPase*,* Z. Naturforsch. C 50 (1995) 660–663. https://doi-org.ezproxy.universite-paris-saclay.fr/10.1515/znc-1995-9-1010.

[49] D. Krstić, K. Krinulović, G. Joksić, V. Spasojević–Tišma, T. Momić, V. Vasić, Effects of Digoxin and Gitoxin on the Enzymatic Activity and Kinetic Parameters of Na^+/K^+-ATPase, J. Enz. Inhib. Med. Chem. 19 (2004) 409–415. https://doi.org/10.1080/14756360410001722065

[50] D. Krstić, K. Krinulović, V. Vasić, Inhibition of Na+/K+-ATPase and Mg^{2+}-ATPase by metal ions and prevention and recovery of inhibited activities by chelators, J. Enz. Inhib. Med. Chem. 20 (2005) 469–476. https://doi.org/10.1080/14756360500213280.

[51] M. Čolović, D. Bajuk-Bogdanović, N. Avramović, I. Holclajtner-Antunović, N. Bošnjaković-Pavlović, V. Vasić, D. Krstić, Inhibition of rat synaptic membrane Na+/K+-ATPase and ecto-nucleoside triphosphate diphosphohydrolases by 12-tungstosilicic and 12-tungstophosphoric acid, Bioorgan. Med. Chem. 19 (2011) 7063–7069. https://doi.org/10.1016/j.bmc.2011.10.008.

[52] J.M. Messmore, R.T. Raines, Decavanadate inhibits catalysis by ribonuclease A, Biochem. Biophys. 381 (2000) 25–30. https://doi.org/10.1006/abbi.2000.1951

[53] R.J. Pezza, M.A. Villarreal, G.G. Montich, C.E. Argarana, Vanadate inhibits the ATPase activity and DNA binding capability of bacterial MutS. A structural model for the vanadate–MutS interaction at the Walker A motif, Nucleic Acids Res. 30 (2002) 4700–4708. https://doi.org/10.1093/nar/gkf606.

[54] M. Aureliano, G. Fraqueza, C.A. Ohlin, Ion pumps as biological targets for decavanadate, Dalton Trans., 42 (2013) 11770-11777. https://doi.org/10.1039/C3DT50462J.

[55] P. Wu, Z. Xiao, J. Zhang, J. Hao, J. Chen, P. Yin, Y. Wei, DMAP-catalyzed esterification of pentaerythritol-derivatized POMs: a new route for the functionalization of polyoxometalates, Chem. Commun. 47 (2011) 5557–5559. https://doi.org/10.1039/c1cc10650c.

[56] Z. Xiao, K. Chen, B. Wu, W. Li, P. Wu, Y. Wei, An Easy Way to Construct Polyoxovanadate-Based Organic–Inorganic Hybrids by Stepwise Functionalization, Eur. J. Inorg. Chem. (2016), 808–811. https://doi.org/10.1002/ejic.201501297

[57] D. Krstić, N. Tomić, K. Krinulović, V. Vasić, The influence of potassium ion (K^+) on digoxin-induced inhibition of porcine cerebral cortex Na^+/K^+-ATPase, J. Enzym. Inhib. Med. Ch. 21 (2006) 471–475. https://doi.org/10.1080/14756360600642230

[58] M.J. Frisch, G.W. Trucks, H.B. Schlegel, G.E. Scuseria, M.A. Robb, J.R. Cheeseman, G. Scalmani, V. Barone, B. Mennucci, G.A. Petersson, H. Nakatsuji, M. Caricato, X. Li, H.P. Hratchian, A.F. Izmaylov, J. Bloino, G. Zheng, J. L. Sonnenberg, M. Hada, M. Ehara, K. Toyota, R. Fukuda, J. Hasegawa, M. Ishida, T. Nakajima, Y. Honda, O. Kitao, H. Nakai, T. Vreven, J.A. Montgomery, J.E. Peralta, F. Ogliaro, M. Bearpark, J.J. Heyd, E. Brothers, K.N. Kudin, V.N. Staroverov, T. Keith, R. Kobayashi, J. Normand, K. Raghavachari, A. Rendell, J. C. Burant, S.S. Iyengar, J. Tomasi, M. Cossi, N. Rega, J.M. Millam, M. Klene, J.E. Knox, J.B. Cross, V. Bakken, C. Adamo, J. Jaramillo, R. Gomperts, R.E. Stratmann, O. Yazyev, A.J. Austin, R. Cammi, C. Pomelli, J.W.

Ochterski, R.L. Martin, K. Morokuma, V.G. Zakrzewski, G.A. Voth, P. Salvador, J.J. Dannenberg, S. Dapprich, A.D. Daniels, O. Farkas, J.B. Foresman, J.V. Ortiz, J. Cioslowski, D.J. Fox, Gaussian, Inc., Wallingford CT, 2010.

[59] A.D. Becke, Density-functional thermochemistry. III. The role of exact exchange**,** J. Chem. Phys. 98 (1993) 5648-5652. https://doi.org/10.1063/1.464913.

[60] Y. Zhao, D.G. Truhlar, The M06 suite of density functionals for main group thermochemistry, thermochemical kinetics, noncovalent interactions, excited states and transition elements: two new functionals and systematic testing of four M06-class functionals and 12 other functionals, Theor. Chem. Acc., 120 (2008) 215−41. http://dx.doi.org/10.1007/s00214-007-0401-8.

[61] J.P. Perdew, Density-functional approximation for the correlation energy of the inhomogeneous electron gas, Phys. Rev. B 33 (1986) 8822–8824. https://doi.org/10.1103/PhysRevB.33.8822.

[62] V.A. Rassolov, M.A. Ratner, J.A. Pople, P.C. Redfern, L.A. Curtiss, 6-31G* basis set for third-row atoms, J. Comp. Chem. 22 (2001) 976–984. https://doi.org/10.1002/jcc.1058.

[63] R.C. Binning, L.A. Curtiss, Compact contracted basis sets for third-row atoms: Ga–Kr, J. Comp. Chem. 11 (1990) 1206-1216. https://doi.org/10.1002/jcc.540111013.

[64] T.H. Dunning, Gaussian basis sets for use in correlated molecular calculations. I. The atoms boron through neon and hydrogen, J. Chem. Phys. 90 (1989) 1007-1023B. https://doi.org/10.1063/1.456153

[65] N.Bošnjaković-Pavlović, A. Spasojević – de Biré, I. Tomaz, N. Bouhmaida, F. Avecilla, U.B. Mioc, J.C. Pessoa, N.E. Ghermani, Electronic properties of a cytosine decavanadate: Toward a better understanding of chemical and biological properties of decavanadates, Inorg. Chem. 48 (2009) 9742–9753. https://doi.org/10.1021/ic9008575

[66] X. Xu, Experimental and theoretical charge density analysis of functionalized polyoxovanadates: toward a better understanding of chemical bonding and chemical reactivity. Other. Ecole Centrale Paris, 2015. English. 〈NNT : 2015ECAP0026〉 〈tel-01181264〉

[67] X. Xu, A. Spasojević-de Biré, N.E. Ghermani, Y. Wei, S. Novaković, N. Bošnjaković-Pavlović, P. Wu, Experimental evidence of charge transfer in a functionalized hexavanadate: a high resolution X-ray diffraction study, Phys.Chem.Chem.Phys., 19 (2017) 18162-18166. https://doi.org/10.1039/c7cp01840a.

[68] Ugo Varetto, Molekel 5.4

[69] T.A. Keith, TK Gristmill Software, AIMALL (Version 14.11.23), Overland Park KS, USA, 2014 (aim.tkgristmill.com).

[70] http://www.moldiscovery.com/software/grid/

[71] E. Carosati, S. Sciabola, G. Cruciani, Hydrogen Bonding Interactions of Covalently Bonded Fluorine Atoms: From Crystallographic Data to a New Angular Function in the GRID Force Field, J. Med. Chem. 47 (21) (2004) 5114–5125. https://doi.org/10.1021/jm0498349.

[72] O. Linnenberg, A. Kondinski, K. Yu. Monakhov, The Lindqvist hexavanadate: A platform for coordination-directed assembly. In Supramolecular Systems: Chemistry, Types and Applications (ed.: C. Pena), Nova Science Publishers, Hauppauge (2017) 39–66.

[73] T. Kurata, A. Uehara, Y. Hayashi, K. Isobe, Cyclic Polyvanadates Incorporating Template Transition Metal Cationic Species: Synthesis and Structures of Hexavanadate [PdV6O18]4-, Octavanadate $[Cu_2V_8O_{24}]^{4-}$, and Decavanadate $[Ni_4V_{10}O_{30}(OH)_2(H_2O)_6]^{4-}$, Inorg. Chem. 44 (7) (2005) 2524-30. https://doi.org/10.1021/ic048751f.

[74] M.I. Khan, Q. Chen, J. Zubieta, D.P. Goshorn, Hexavanadiuin polyoxo lkoxide anion clusters: Structures of the mixed-valence species

$(Me_3NH)[V^{IV}_5V^{V}O_7(OH)_3\{CH_3C(CH_2O)_3\}_3]$ and of the reduced complex $Na_2[V^{IV}_6O_7\{CH_3CH\ 2C(CH_2O)_3\}_4]$, Inorg. Chem. 31 (1992) 1556–1558. https://doi.org/10.1021/ic00035a007.

[75] J. Spandl, C. Daniel, I. Brudgam, H. Hartl, Synthesis and structural characterization of redox-active dodecamethoxoheptaoxohexavanadium clusters, Angew. Chem. Int. Ed. 42 (2003) 1163–1166. https://doi.org/10.1002/anie.200390306.

[76] N. Bošnjaković-Pavlović, J. Prévost, A. Spasojević-de Biré, Crystallographic Statistical Study of Decavanadate Anion Based-Structures: Toward a Prediction of Noncovalent Interactions, Crystal Growth & Design 11 (9) (2011) 3778-3789. https://pubs.acs.org/doi/10.1021/cg200236d.

[77] L.C. Cantley, L. Josephson, R. Warner, M. Yanacisawa, C. Lechene, G. Guidotti. Vanadate is a potent (Na, K)-ATPase inhibitor found in ATP derived from muscle, J. Biol. Chem. 252 (1977) 7421–7423. http://www.jbc.org/content/252/21/7421.

[78] W. Kühlbrandt, Biology, structure and mechanism of P-type ATPases". Nat. Rev. Mol. Cell Biol. 5 (4): (2004) 282–295. https://doi.org/10.1038/nrm1354

Table caption

Table 1. The inhibition parameters of hexavanadates for Na^+/K^+ - ATPase obtained by Hill analysis; IC_{50} is the concentration of the investigated compounds with capability to inhibit 50% of the enzyme activity.

Table 2. Geometrical, MIF and inhibition parameters of V_{10} and a set of functionalized V_6. Compounds are separated in three groups (between the bold lines) V_{10}, short V_6, long V_6. Number of carbon atoms (second column) and heteroatoms (third column) contained in the organic chain. Geometrical parameters: longest length between two atoms of the organic chain

(fourth column); volume (fifth column) and area (sixth column) occupied by the electron density at the molecular surface (0.00007 eA^{-3}) as determined via *ab initio* calculations. MIF parameters: area (seventh column) of the negative surface at -2 $kcal.mol^{-1}$ for V_6 and -0.7 $kcal.mol^{-1}$ for V_{10}; ratio (eighth column) of the MIF negative iso-surface over molecular surface area. IC_{50} inhibition parameters (M): the different columns correspond to the different cations used to stabilize the anions in the inhibition experiments. Some values have already been published and are indicated [a] [44] [b] [45].

Table 3. Summary of the inhibition results or predictions obtained with the different methods used in this work.

Figure caption

Figure 1. (a) Concentration-dependent inhibition of Na^+/K^+-ATPase activity induced by three functionalized hexavanadates. The values are expressed as mean ± S.E.M; (b) Hill analysis of $Na^{+/}K^+$-ATPase activity inhibition induced by three functionalized hexavanadates.

Figure 2. Experimental, theoretical electrostatic potential (EP) and molecular interaction field (MIF) with water probe on anion **10**. Experimental EP (**10**-Cyt) is reproduced with permission of reference [65].

Figure 3. Electrostatic potential (EP) (Gaussian/M06/cc-pVTZ) and molecular interaction field (MIF), water probe on anion **1**. EP is reproduced with permission of reference [45].

Figure 4. Electrostatic potential (EP) (Gaussian/M06-2X/cc-pVTZ) and molecular interaction field (MIF), water probe on anion **7**. EP is reproduced with permission of reference [45].

Figure 5. Electrostatic potential (EP) (Gaussian/M06-2X/cc-pVTZ) and molecular interaction field (MIF), water probe on anion **2**. EP is reproduced with permission of reference [45].

Figure 6. Electrostatic potential (EP) (Gaussian/M06-2X/cc-pVTZ) and molecular interaction field (MIF), water probe on anion **9**.

Figure 7. Comparison of experimental inhibition parameter (IC_{50} * 1000) for the V_6 compounds stabilized with TBA as a counter cation with the ratio (eighth column of Table 2) of the MIF negative iso-surface over molecular surface area (criterion V). The organic ligand is given besides the anion number. Two colored lines indicates the trend. Compounds were ranked according to their ratio values. When the value does not exist the compounds have been inserted according to their IC_{50} value. Criteria on the negative extension of negative EP criterion I) or MIF iso-surface (criterion III) are indicated on the right part of the figure. It has to be noticed that due to the construction of this figure, one cannot predict the relative inhibition potential between the group **4** > **9** > **5** and **3** which could be inserted at any position in this series in this ranking.

Table 1.

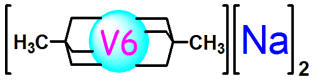
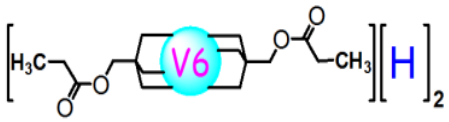
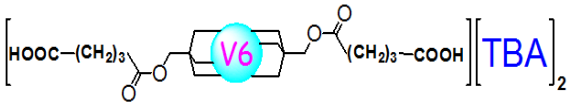
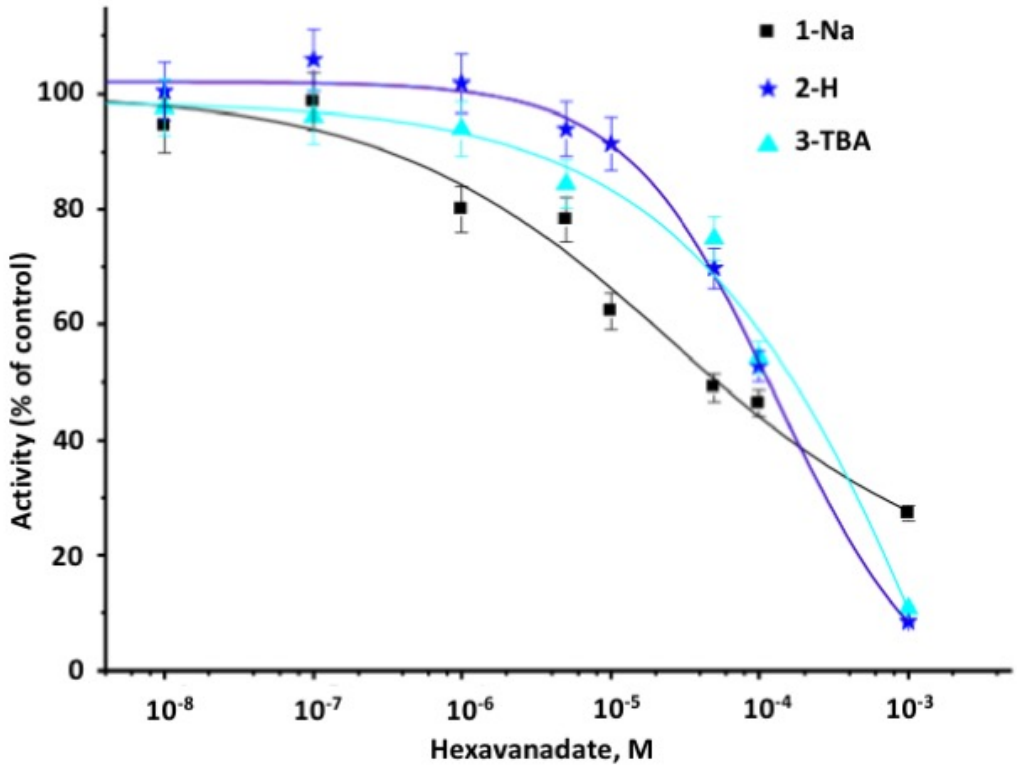
Compound	Structure of functionalized hexavanadates	IC_{50}, M	n_H
1-Na		$(5.50 \pm 0.28) \times 10^{-5}$	0.44
2-H		$(1.05 \pm 0.05) \times 10^{-4}$	0.98
3-TBA		$(1.31 \pm 0.06) \times 10^{-4}$	0.99

Table 2.

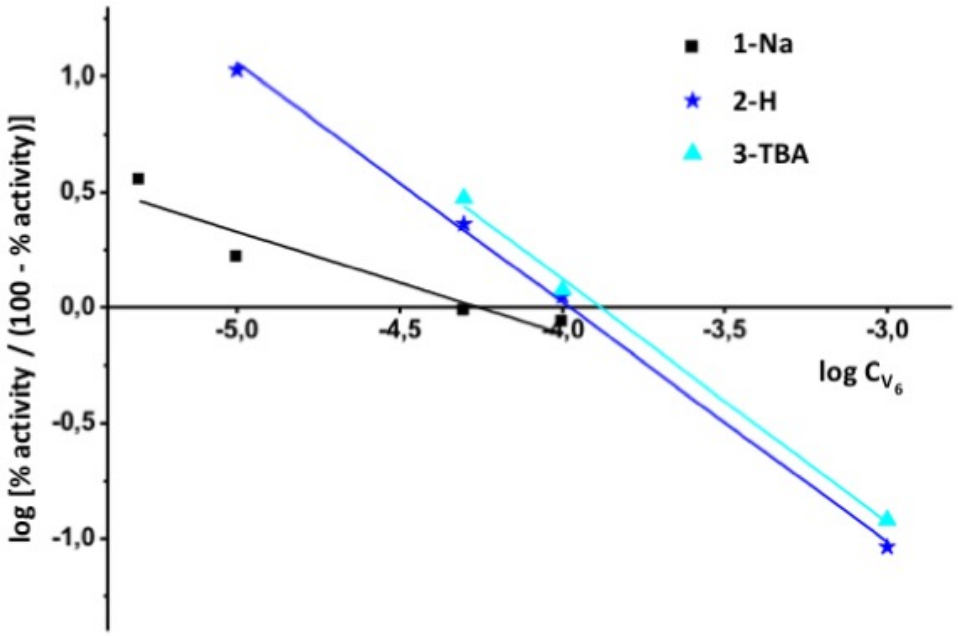
Compound			Geometrical parameters			MIF		IC_{50}			
anion	Num. C	Num N or O	length (Å)	Volume ($Å^3$)	Area ($Å^2$)	Area ($Å^2$)	ratio	TBA	Na	H	NH_4
10	0	0	9.9	655	542	644	1.19				$1.71*10^{-06}$ *b*
6	0	1	11.1	323	495	559	1.13				
1	1	0	11.3	316	334	212	0.63	0.000076 *a*	0.000055		
7	0	3	12.5	355	512	538	1.05	0.000018 *a*			
8	1	1	12.9	354	498			0.000029 *a*	>0.001 *a*		
2	4	2	16.5	467	737	555	0.75	0.000055 *a*		0.000105	
4	7	2	16.7	1074	944	573	0.61				
3	5	4	18.5	498	786			0.000131			
9	16	5	27.3	916	1396	773	0.55				
5	19	2	54.7	1355	1849	562	0.30				

Table 3

Criteria			Favorable	Unfavorable	Non tested
Exp.	**IC_{50}**	(all compounds)	**10-NH_4 >> 7-TBA** > **8-TBA** > **1-TBA** > **2-TBA** > **1-Na** ~ **2-H** > **3-TBA** > **8-Na**		**4-TBA**, **5-TBA**, **6-TBA**, **9-TBA** and **10-Cyt**
EP	**I**	EP extension	**6**, **7** and **8**	**1**, **2**, **4**, **5** and **9**	**3**
	II	Atomic net charges	no effect		**3** and **5**
MIF	**III**	MIF extension	**2**, **4**, **6**, **7** and **9**	**1** and **5**	**8** and **3**
	IV	MIF surface	**9** >> **10** >> **4** > **5** ~ **6** ~ **2** >> **1**		
MIF + molecular surface	**V**	ratio	**10** > **6** > **7** > **2** > **1** > **4** > **9** > **5**		**8** and **3**


1-Na
2-H
3-TBA
Activity (% of control)
100
80
60
40
20
0
10^{-8}
10^{-7}
10^{-6}
10^{-5}
10^{-4}
10^{-3}
Hexavanadate, M

a)


1-Na
2-H
3-TBA
log [% activity / (100 - % activity)]
1,0
0,5
0,0
-0,5
-1,0
-5,0
-4,5
-4,0
-3,5
-3,0
log C_{V_6}

b)

Figure 1

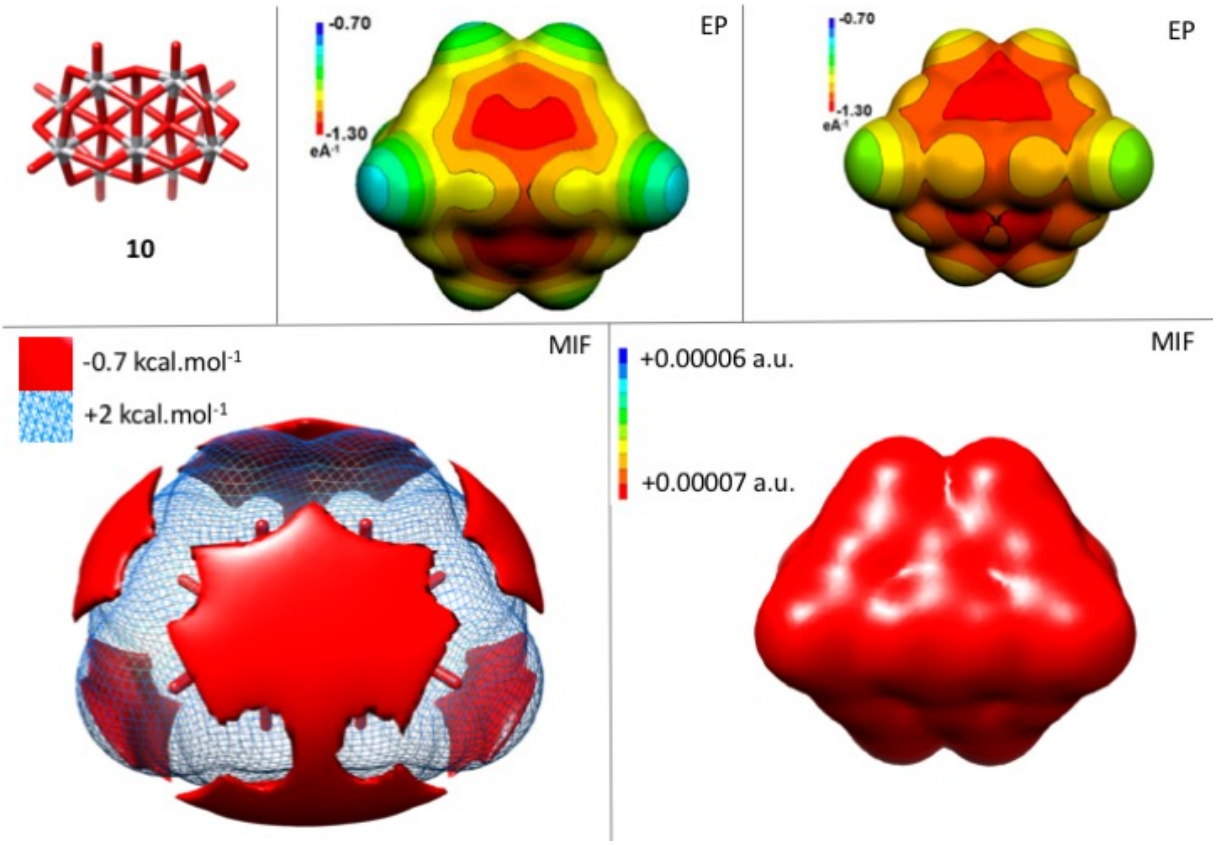

10
-0.70
-1.30
eA-1
EP
-0.70
-1.30
eA-1
EP
-0.7 kcal.mol-1
+2 kcal.mol-1
MIF
+0.00006 a.u.
+0.00007 a.u.
MIF

Figure 2.

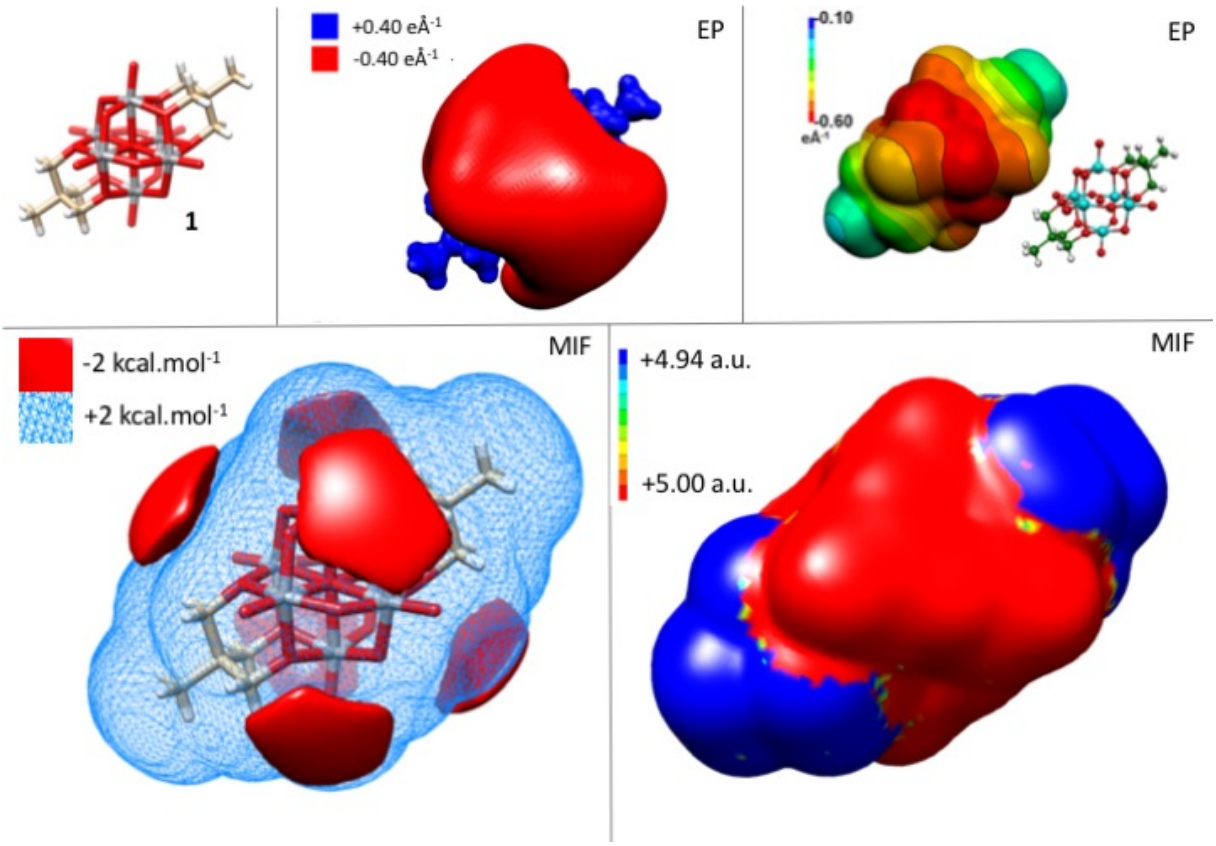

1
+0.40 eÅ-1
-0.40 eÅ-1
EP
0.10
-0.60
eÅ-1
EP
-2 kcal.mol-1
+2 kcal.mol-1
MIF
+4.94 a.u.
+5.00 a.u.
MIF

Figure 3.

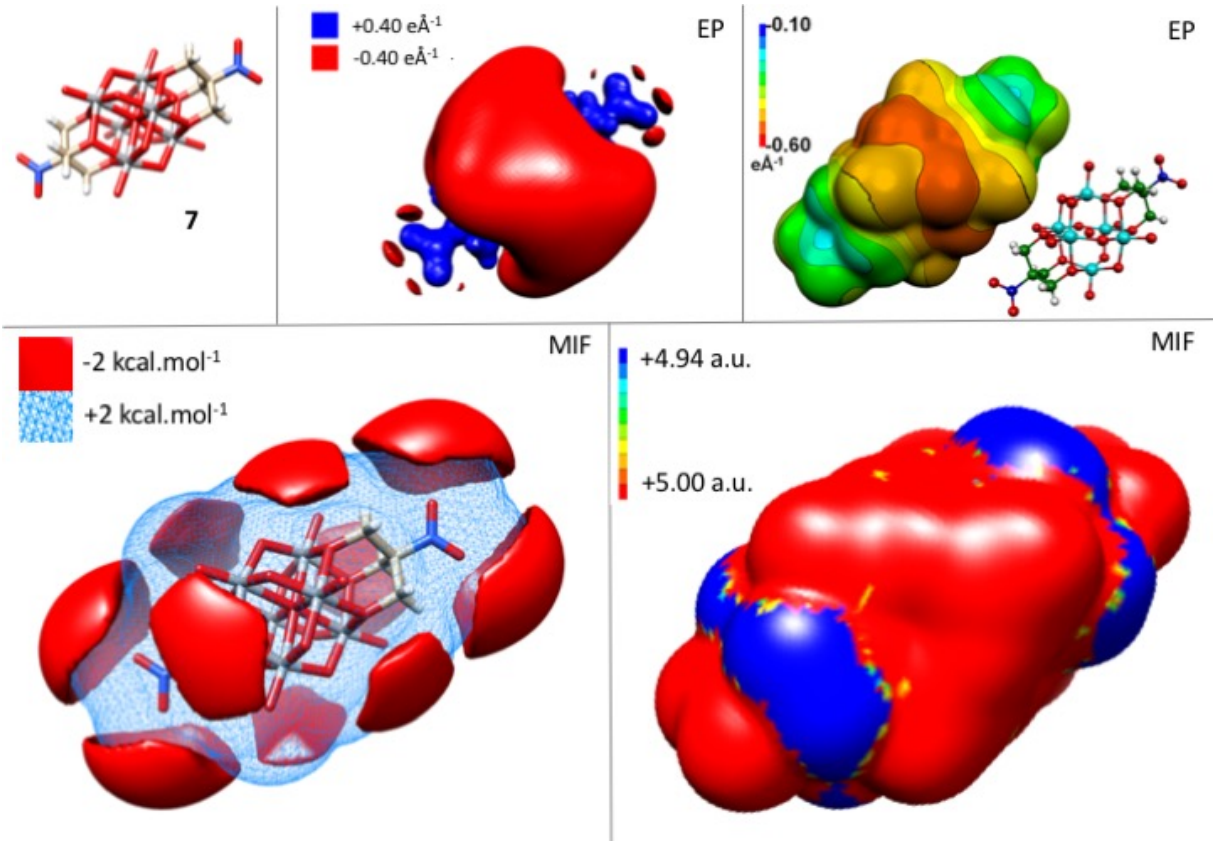

7
+0.40 eÅ-1
-0.40 eÅ-1
EP
0.10
-0.60
eÅ-1
EP
-2 kcal.mol-1
+2 kcal.mol-1
MIF
+4.94 a.u.
+5.00 a.u.
MIF

Figure 4.

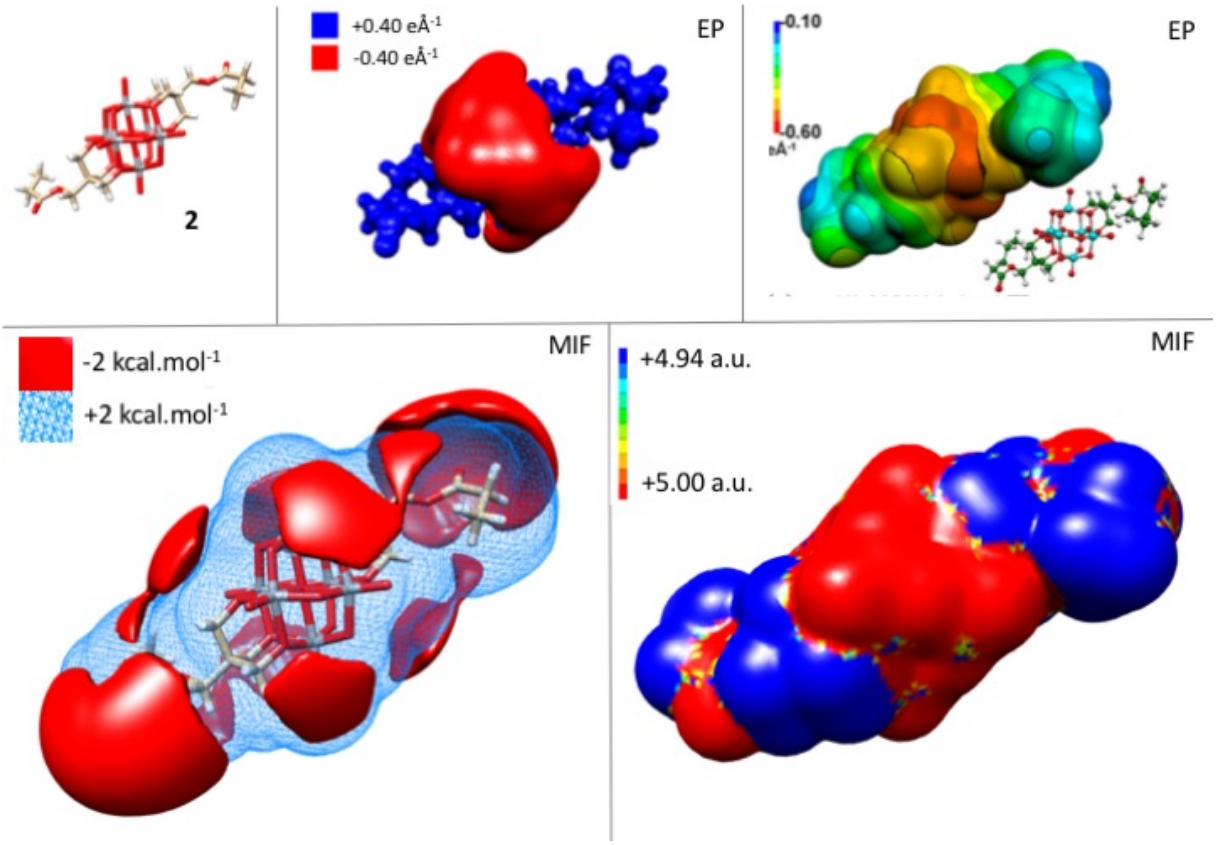

2
+0.40 eÅ-1
-0.40 eÅ-1
EP
0.10
-0.60
eÅ-1
EP
-2 kcal.mol-1
+2 kcal.mol-1
MIF
+4.94 a.u.
+5.00 a.u.
MIF

Figure 5.

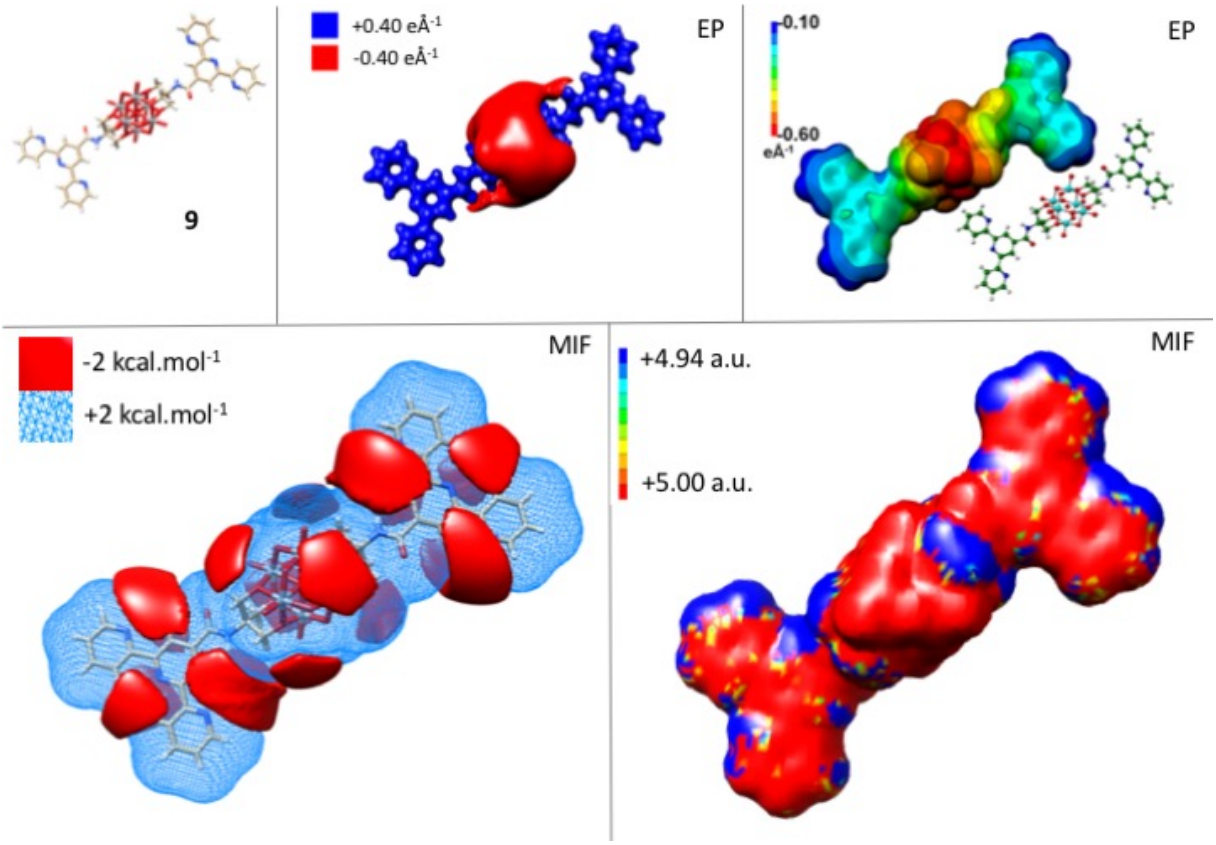

9
+0.40 eÅ-1
-0.40 eÅ-1
EP
0.10
-0.60
eÅ-1
EP
-2 kcal.mol-1
+2 kcal.mol-1
MIF
+4.94 a.u.
+5.00 a.u.
MIF

Figure 6.

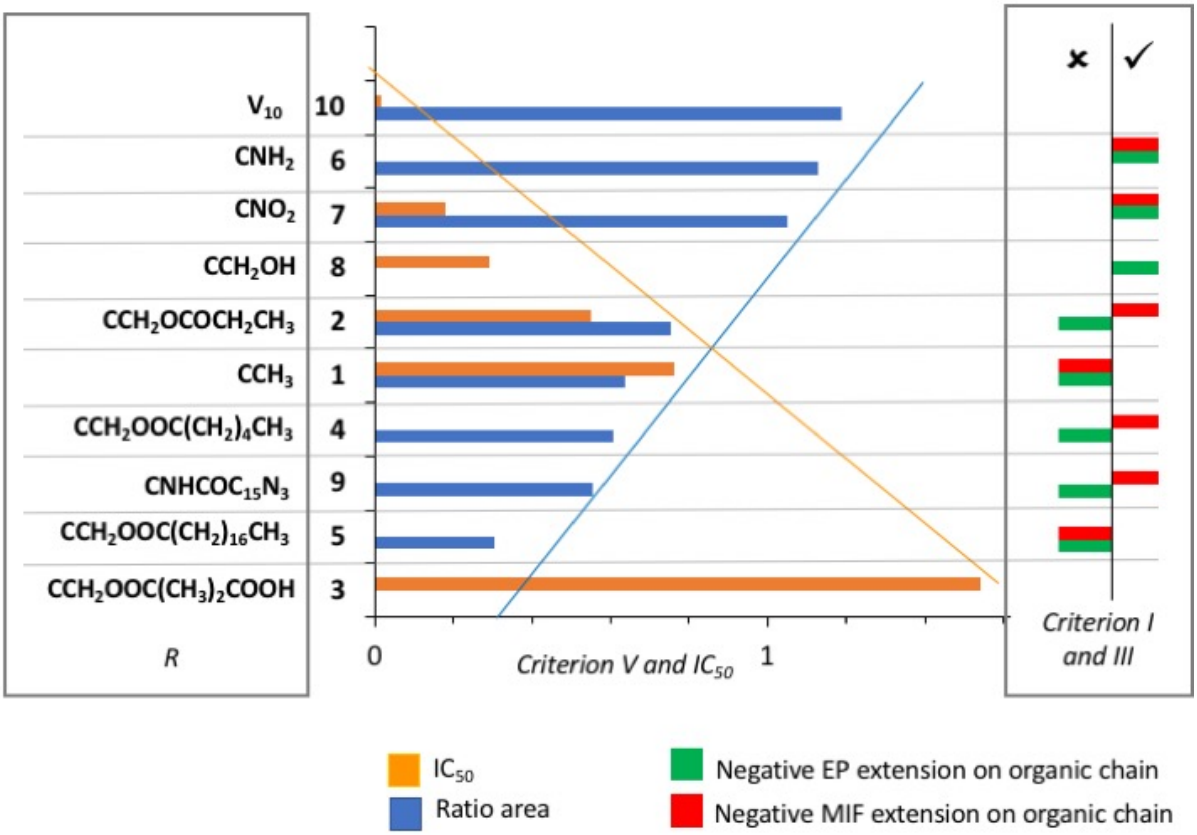

V10
CNH2
CNO2
CCH2OH
CCH2OCOCH2CH3
CCH3
CCH2OOC(CH2)4CH3
CNHCOC15N3
CCH2OOC(CH2)16CH3
CCH2OOC(CH3)2COOH
R
10
6
7
8
2
1
4
9
5
3
0
1
Criterion V and IC50
×
✓
Criterion I and III
IC50
Ratio area
Negative EP extension on organic chain
Negative MIF extension on organic chain

Figure 7.